Hindawi Publishing Corporation
International Journal of Photoenergy
Volume 2014, Article ID 542658, 8 pages
http://dx.doi.org/10.1155/2014/542658

Research Article

Mechanooptic Regulation of Photoconduction in Functionalized Carbon Nanotubes Decorated with Platinum

C. Mercado-Zúñiga,[1,2] C. Torres-Torres,[1] M. Trejo-Valdez,[3] R. Torres-Martínez,[4] S. Tarrago-Velez,[5] F. Cervantes-Sodi,[5] and J. R. Vargas-García[2]

[1] *Sección de Estudios de Posgrado e Investigación, ESIME ZAC, Instituto Politécnico Nacional, 07738 México, DF, Mexico*
[2] *Departamento de Ingeniería Metalurgia y Materiales, ESIQIE, Instituto Politécnico Nacional, 07300 México, DF, Mexico*
[3] *Instituto Politécnico Nacional, ESIQIE, 07738 México, DF, Mexico*
[4] *Centro de Investigación en Ciencia Aplicada y Tecnología Avanzada Unidad Querétaro, Instituto Politécnico Nacional, 76090 Santiago de Querétaro, QRO, Mexico*
[5] *Departamento de Física y Matemáticas, Universidad Iberoamericana, Prolongación Paseo de la Reforma 880, Lomas de Santa Fe, 01219 México, DF, Mexico*

Correspondence should be addressed to C. Torres-Torres; crstorres@yahoo.com.mx

Received 6 February 2014; Accepted 8 April 2014; Published 9 June 2014

Academic Editor: Xie Quan

The observation of photoconduction and nonlinear optical absorption on functionalized multiwall carbon nanotubes decorated with platinum is reported. The samples were prepared by a chemical vapor deposition method. The electrical conductivity of the carbon nanotubes seems to be decreased by the functionalization process; but this property is strongly enhanced after the incorporation of platinum particles. Nonresonant photoconductive experiments at 532 nm and 445 nm wavelengths allow us to detect a selective participation of the platinum to the photoelectrical response. A mechanooptic effect based on Fresnel reflection was obtained through a photoconductive modulation induced by the rotation of a silica substrate where the samples were deposited as a thin film. A two-photon absorption process was identified as the main physical mechanism responsible for the nonlinear optical absorption. We consider that important changes in the nonlinear photon interactions with carbon nanotubes can be related to the population losses derived from phonons and the detuning of the frequency originated by functionalization.

1. Introduction

One of the most significant scientific interests related to studying carbon nanostructures comes from their particular advantages for designing nanosystems that can be improved by a number of materials [1]. Among some examples devoted to investigating highly sensitive instrumentation of signals, diverse reports have been dedicated to describing mechanical [2–5] or electrical [6–8] tasks that highlight the extraordinary properties exhibited by carbon nanotubes (CNTs).

Several preparation methods for evaluating the morphological and structural characteristics of CNTs have been carried out [9, 10]; and also the possibility of influencing the resulting physical functions of advanced materials based on CNTs seems to be attractive [11]. Moreover, it is notable that the adjustment of singular physical features during the processing route of different samples has been accomplished by implementing hybrid organic-inorganic materials mainly constituted by CNTs [12–15].

In many fields of nanotechnology, distinct kinds of CNTs have drawn considerable attention regarding their outstanding optical and electrical parameters [16, 17]. In addition, the great importance of the third order optical nonlinearities of CNTs has also originated to consider them as exceptional materials for proposing all-optical systems displaying powerful absorptive and refractive nonlinear effects [18–22]. Apparently, the development of nonlinear low-dimensional compound materials is a crucial step towards the improvement of all-optical nanotechnology [23]. So, in regard to the fascinating mechanical, optical, and electrical response

associated with CNTs, an opportunity to use them for developing multifunctional smart materials can be contemplated.

The research progress of the photoconductive and mechanooptical response of CNTs and other metal elements has originated that different configurations can be considered as ideal candidates for next-generation of flexible transparent conducting films [24]. Decoration of CNTs by metallic nanoparticles (NPs) is attractive because the resulting physical characteristics exhibited by the individual components can be enhanced [25–27]. Using electrochemical deposition methods, a good control on size and densities of Pt NPs or bimetallic Pt-Ru NPs decorating CNTs has been accomplished [28, 29]. On the other hand, microwave-assisted hydrothermal synthesis has allowed the preparation of Pd NPs, Ni NPs, and Sn NPs decorated on CNTs [30]. Following a polyol process, homogeneous distributions of Au NPs, Ag NPs, Pt NPs, and Pd NPs, as well as bimetallic PtPd NPs and Pt-Ru NPs, have been deposited on CNTs [31–35]. And it has been pointed out that the optical transmittance and electrical conductivity of the resulting samples can be controlled by the deposition time of the processing route [35]. Moreover, in order to form heterojunctions of CNTs to metal NPs, electron-beam systems have been employed [36–38], and Fe NPs, Co NPs, Ni NPs, and FeCo NPs, decorating CNT with improved electrical and mechanical properties, have been obtained [39].

With this motivation, in this research an attempt has been made to further investigate the potential applications of the photoconductive and mechanooptic response of multiwall CNTs (MWCNTs). Experimental results associated with functionalization, electrical, photoconductive, and nonlinear optical absorption phenomena that were successfully enhanced by platinum decoration of the studied samples are presented.

2. Experimental Details

2.1. MWCNTs: Synthesis and Functionalization. MWCNTs were produced by thermal decomposition of Toluene (Fermont, 99.9% purity) and Ferrocene (Sigma-Aldrich, 98% purity) in a tubular reactor at $T = 850^{\circ}C$, $P_{tot} = 80.1$ kPa for 40 min. Ferrocene was dissolved in Toluene to form the source solution in a 1/39 moL ratio. The solution was nebulized as microdroplets and carried into the reactor by Ar gas with a flow rate of 2.5 L/min. [40]. MWCNTs were functionalized in 3 : 1 v/v mixture of sulfuric (30 mL, 95–97%) and nitric acid (10 mL, 65%) under sonication (42 kHz) for 15 min at room temperature. After functionalization, MWCNTs were repeatedly washed in distilled water, centrifuged, and dried in vacuum [41]. The quality of functionalized MWCNTs (f-MWCNTs) was investigated by Raman Spectroscopy (Jobin Yvon Horiba).

2.2. Incorporation of Metal NPs on f-MWCNTs. The f-MWCNTs decorated with platinum particles (Pt/f-MWCNTs) were prepared by an *in situ* vapor-phase grafting process of Pt acetylacetonate [$(CH_3\text{-}COCHCO\text{-}CH_3)_2Pt$ Aldrich, 97%] in a quartz tube reactor at total pressure of 0.26 kPa. Pt-acac was decomposed into two sequential thermal steps: the first at 180°C for 600 s and the second at 400°C for 600 s in a different reactor segment.

Afterwards, the resulting samples were suspended in an ethanol solution contained in a quartz cuvette with 1 mm width. The concentration of the solution was heuristically chosen for a better observation of the optical absorption bands that correspond to the plasmonic response of the samples in their linear optical spectra. Then, the obtained liquid solutions were deposited by dripping on different SiO_2 substrates, deriving from selected thin film samples with a resulting thickness of approximately 1 μm. The thin films were used for performing the electrical measurements and the nonlinear optical experiments.

2.3. Photoconductive Measurements. Electrical measurements were evaluated using an Autolab/PGSTAT302N high power potentiostat/galvanostat. The impedance spectrum was measured with a 10 mV signal and an integration time of 1 s. The photoconduction on the samples was separately investigated at 445 nm and 532 nm wavelengths with continuous wave (CW) lasers providing 1 W of average power. The incident polarization of the optical beam was aligned to coincide with the path in measurement. The electrodes used for these experiments were in direct contact with the sample; they were located in the neighborhood of the diameter of the incident beam. The conductivity was measured using two metallic electrodes separated by a distance of 5 mm for each studied sample.

2.4. Linear Optical Response. The linear absorption spectrum of the samples was acquired with a Perkin Elmer XLS UV-visible spectrophotometer.

2.5. Photoconduction and Nonlinear Optical Response. The optical transmittance and photoconduction in the thin films were measured by means of a high irradiance single beam transmittance experiment. A 532 nm wavelength with 1 ns pulse duration was monitored using the second harmonic of a Nd-YAG laser source continuum model SL II-10.

2.6. Mechanooptic Regulation of Photoconduction. Considering the possibility of promoting controlled contributions of light for inducing a photoconduction behavior in the sample, we proposed the optoelectronic system assisted by a mechanical actuator illustrated in Figure 1. The rotation of the sample generates a change in the transmitted light through the SiO_2 substrate due to Fresnel reflection. So, the variation in the incident light on the Pt/f-MWCNTs allows a modification in the resulting photoconductive effect.

3. Results and Discussion

Figure 2 shows the Raman spectra of the studied pristine and f-MWCNTs. Three characteristic peaks are clearly observed: the D band (~1334 cm^{-1}), the G band (~1580 cm^{-1}), and the G' band (~2660 cm^{-1}). The intensity ratio of the D and G bands ($I_{D/G}$) was estimated to be 0.68 for pristine MWCNTs

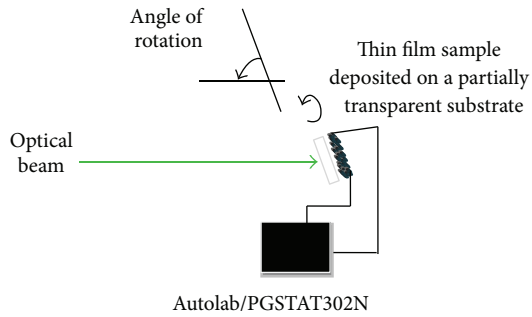

Figure 1: Setup for implementing a mechanooptic modulation of photoconduction.

and 0.38 for f-MWCNTs. As the D and G bands are indicative of defects and graphitic structure, respectively, the decrease in the $I_{D/G}$ ratio was interpreted as a reduction of defects in the f-MWCNTs. In addition, the increase in the G' band intensity for f-MWCNTs was consistently related to a decrement of defects and impurities [42].

A representative field emission scanning electron microscopy (FE-SEM) image of Pt/f-MWCNTs is shown in Figure 3. Pt particles are uniformly distributed on the external surface of nanotubes. In this sample, energy-dispersive X-ray spectroscopy (EDX) analysis indicated that Pt content was about 5 wt%. High resolution transmission electronic microscopy (HRTEM) observations (inset) revealed that Pt particles have a mean size of 2.3 nm.

It has been previously reported that the incorporation of Pt will increase the conductivity exhibited by decorated carbon nanotubes [43]. The electrical results for our studied samples are shown in Figure 4. As it could be expected, a considerable enhancement in the resulting alternating current (AC) was derived from the incorporation of Pt in the nanotubes. But it is worth noting that the functionalization of the tubes originates a remarkable inhibition of the conductive response, probably because this process may promote the quenching of free holes that generates a change in the conductive phenomena.

Photoconductive results were obtained in darkness and under 532 nm wavelength of irradiation on the samples. The experimental data are presented in Figure 5. While photoconduction was observed for the undecorated MWCNTs, no photoconduction was detected for the f-MWCNTs, but a redistribution of the charges in the resistive model together with a change in capacitance was present.

Comparatively, photoconductive explorations carried out in the samples by a 445 nm irradiation seem to activate the photoconductive response in the f-MWCNTs as it can be observed from Figure 6. An evident change in the electric signals can be observed by comparing the different conditions of photonic excitation.

The fitting of the experimental data shown in Figures 4–6 was achieved by numerical simulations considering Ohm's law and the following expression:

Table 1: Electrical parameters in the studied samples.

Experiment	R_1 (Ω)	R (Ω)	C (pF)
MWCNTs in darkness	260000	639594	3
MWCNTs under 532 nm irradiation	170000	659594	5
MWCNTs under 445 nm irradiation	185000	630000	5.5
f-MWCNTs in darkness	410000	809594	1.6
f-MWCNTs under 532 nm irradiation	899594	440000	6
f-MWCNTs under 445 nm irradiation	385000	1000000	7
Pt/f-MWCNTs in darkness	199000	639594	6
Pt/f-MWCNTs under 532 nm irradiation	220000	439594	11
Pt/f-MWCNTs under 445 nm irradiation	170000	500000	5

$$|Z| = \frac{R_1\sqrt{R^2 + {X_C}^2}}{R_1 + \sqrt{R^2 + {X_C}^2}}, \quad (1)$$

where $X_C = -j/\omega C$, $j = \sqrt{-1}$, ω is the angular frequency of the AC of electrons, R and R_1 represent the electric resistances, X_C is the capacitive reactance, and C is the capacitance. Best fitting parameters are presented in Table 1.

Taking into account the data described in Table 1, for the higher electrical frequencies plotted in Figures 5 and 6, the photoconductive response in the Pt/f-MWCNTs shows a stronger capacitance behavior associated with the change in their monotonical increase in conductivity. This behavior is consistent with the fact that some electrical charges could be stored by the excitation of Pt ions that are also incorporated in the tubes. Regarding these photoconductive results, it can be considered that the functionalization ought to originate a modification of metastable electronic states that results in a decrease of the conductivity.

On the other hand, the experimental setup illustrated in Figure 1 was implemented in order to explore the possibility of developing a mechanooptic sensor assisted by photoconduction. The response of the system was based on the photoconductive properties of the Pt/f-MWCNTs deposited on a SiO_2 substrate under a 445 nm irradiation with 1 W average power. In Figure 7 are plotted the experimental results acquired as a function on the angle of rotation.

To better describe the contribution of multiphotonic interactions in the electrical measurements, a quantification of the linear and nonlinear optical response of the samples was undertaken. Similar optical spectra were obtained for studied samples with equivalent amounts of MWCNTs, f-MWCNTs, or Pt/f-MWCNTs. Figure 8 depicts a representative linear absorption spectrum exhibited by the Pt/f-MWCNTs sample. One can clearly see at the plot,

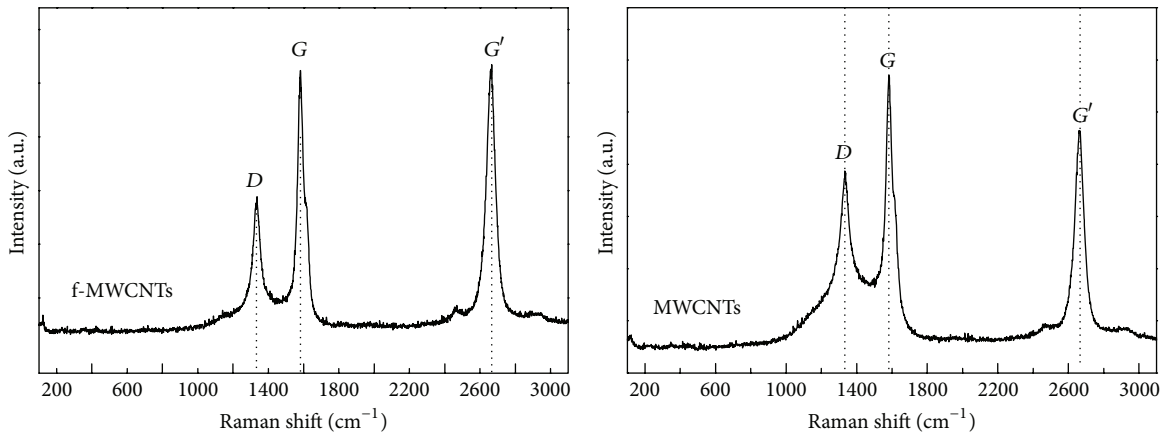

Figure 2: Raman spectra of pristine and functionalized nanotubes (f-MWCNTs).

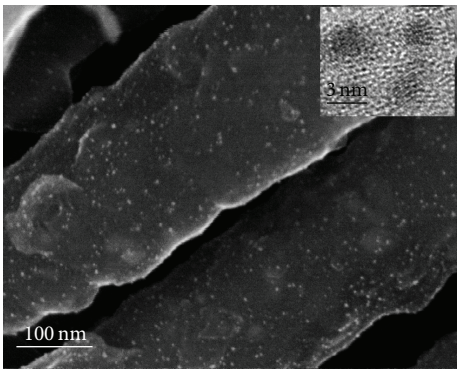

Figure 3: Field emission-SEM image of Pt/f-MWCNTs.

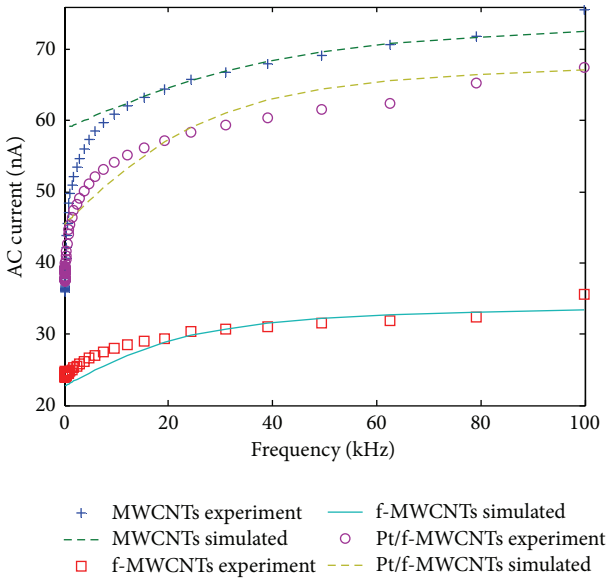

Figure 5: Photoconductive response under 532 nm irradiation as a function of electrical frequency.

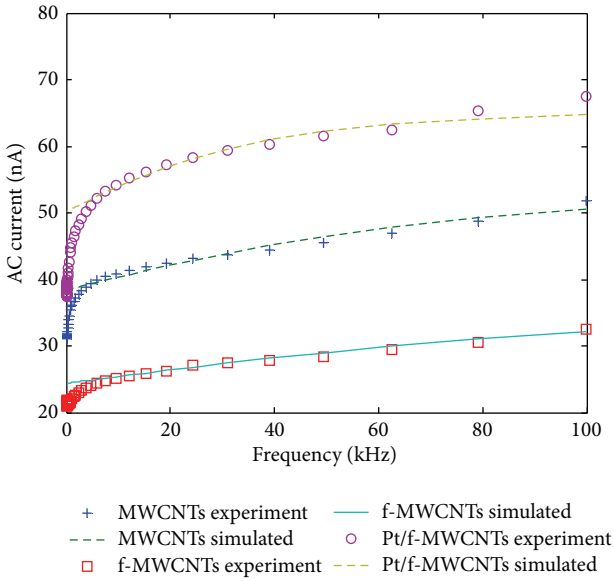

Figure 4: Electrical response of the studied samples as a function of electrical frequency.

close to 270 nm wavelength, an absorbing band associated with the plasmonic response of the studied samples.

A high irradiance optical beam at 532 nm wavelength was selected to observe if any involvement of multiphotonic interaction could be discerned during the propagation of a nonresonant optical beam. Figure 9 illustrates the obtained results; a noticeable modification in the transmittance for the Pt/f-MWCNTs can be clearly distinguished.

The fit of the nonlinear optical transmittance was performed using the expression for the transmitted irradiance $I(L)$ in the presence of nonlinear optical absorption:

$$I(L) = \frac{I_0 \exp(-\alpha_o L)}{1 + \beta I_o L_{\text{eff}}}, \quad (2)$$

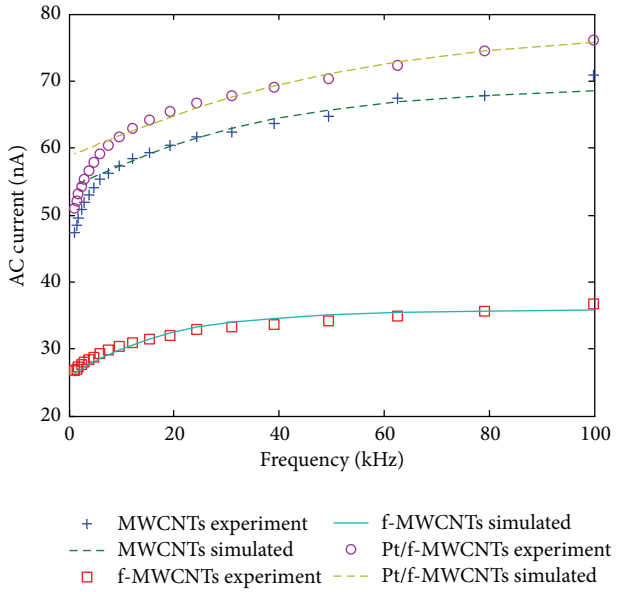

Figure 6: Photoconductive response under 445 nm irradiation as a function of electrical frequency.

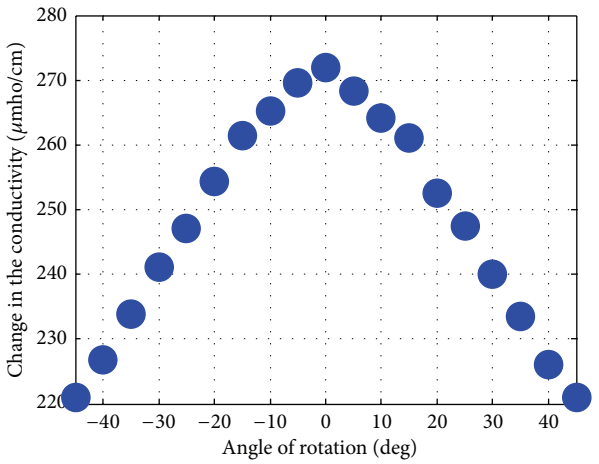

Figure 7: Photoconductive response in the studied Pt/f-MWCNTs as a function of the angle of rotation of the supporting substrate.

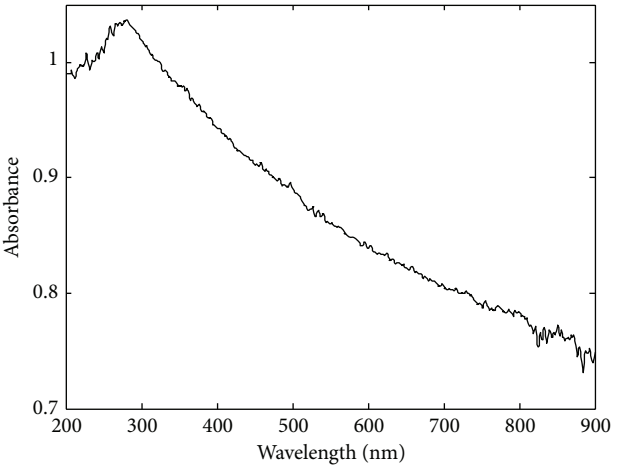

Figure 8: Linear optical absorption spectrum of Pt/f-MWCNTs.

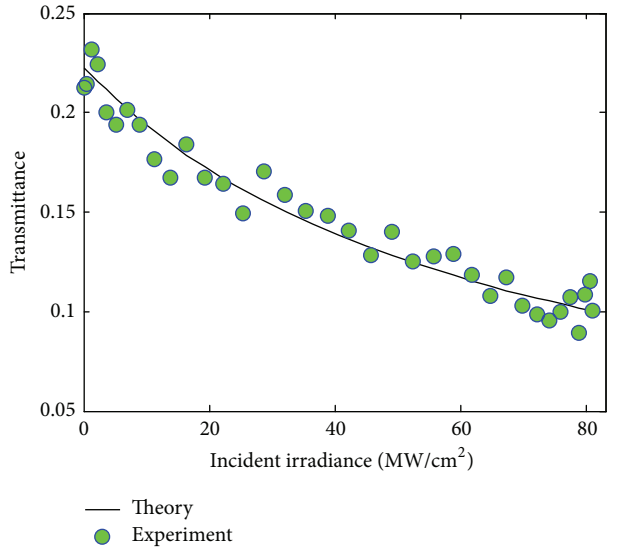

Figure 9: Nonlinear optical transmittance exhibited by Pt/f-MWCNTs.

where β represents the nonlinear absorption coefficient, I_o is the total irradiance of the incident beam, L_{eff} is the effective length given by $L_{\text{eff}} = (1-e^{-\alpha_o L})/\alpha_o$, with L the sample length, and α_o is the linear absorption coefficient.

The best fitting for the linear and nonlinear absorptive coefficients for the samples results in $\alpha_0 = 15\,\text{cm}^{-1}$ and $\beta = 1.51 \times 10^{-7}$ cm/W for the Pt/f-MWCNTs case. The error bar in the experimental data is around ±5%. A typical behavior of a two-photon absorption (TPA) effect in Pt/f-MWCNTs is evidently described by the transmittance results plotted in Figure 9. This TPA phenomenon, together with the enhancement in the photoconductivity at higher repetition rates of nanosecond pulses, could be associated with an important contribution of multiphotonic interactions that results after the incorporation of Pt in the tubes.

In order to explain the observed nonlinear optical response, we considered the dipole approximation in a system of N two-level atoms per unit volume under a high optical irradiance. Then, in the limit of large detunings, that is, $T_2\Delta \gg 1$, it can be demonstrated that the real and imaginary part of the third order optical susceptibility, $\chi^{(3)}$, can be written as [44, 45]

$$\text{Re}\,\chi^{(3)} \approx \frac{4}{3}Nm^4\left[\frac{1}{\hbar\Delta}\right]^3\frac{T_1}{T_2}, \tag{3}$$

$$\text{Im}\,\chi^{(3)} \approx -\frac{4}{3}Nm^4\left[\frac{1}{\hbar\Delta}\right]^3\frac{T_1}{T_2^2\Delta}, \tag{4}$$

where m represents the atomic dipole moment, $\Delta = \omega - \omega_{21}$ is the detuning of the frequency ω of the incident radiation, $1/T_1$ represents the population loss through radiative and nonradiative processes of the upper level, and $1/T_2$ represents

the rate of polarization loss for the off-diagonal matrix elements. From (3) and (4) it is possible to observe an evident influence of the temporal radiative and nonradiative processes on the third order optical response. Under nonresonant conditions, the nonradiative spontaneous emission of the atoms would be much smaller than both the radiative spontaneous emissions; nevertheless, a modification in the optical nonlinearities is expected for important changes in the nonlinear photon interactions mainly related to the population losses derived from phonons and the detuning of the frequency originated by functionalization.

For further investigation of the participation of optical absorption in the physical mechanism responsible for the photoconductivity, we irradiated the samples by employing optical pulses at 532 nm with about 50 MW/cm^2 at 1 Hz repetition rate provided by our Nd-YAG system. The data shown in Figure 10 correspond to 5 optical pulses and the results point out an important change in the photoconduction dependent on the incident pulses. Experimental observations compared to previous reports [46] reveal that a noticeable participation of a thermal effect could be expected to activate an additional conductive effect into our samples as it can be seen from Figure 10.

We calculated the heat-transference generated by optical irradiation in propagation through the sample by using [47],

$$\frac{\partial T}{\partial t} = \frac{\partial}{\partial z}\left[\frac{\kappa}{\rho C}\frac{\partial T}{\partial z}\right] + \frac{\alpha}{\rho C} I(t,z), \quad (5)$$

where T is the temperature, which is a function of the estimated depth in our sample $z = 1\,\mu$m. As a first approximation, we considered the thermal conductivity $\kappa = 200\,\text{W/m}^\circ\text{K}$, the density $\rho = 1 \times 10^{-3}\,\text{Kg/cm}^3$, and the heat capacity $C = 1 \times 10^3\,\text{J/Kg}^\circ\text{K}$ for MWCNTs previously reported [48]. In our case the time of irradiation $t = 5$ s, the linear absorption coefficient $\alpha = 2 \times 10^6\,\text{m}^{-1}$, and I is the optical intensity. The estimated results indicate that an instantaneous temperature change of approximately 180° K can be expected after the propagation of each pulse. However experimental measurements allow us to state that long duration temperature changes (after at least one second) of about 2° K were detected in agreement with our calculations.

The possibility of enhancing the nonlinear optical response and the electronic features of CNTs samples by the modification of metastable electronic levels appears to be attractive. What is more, we consider that potential applications for tailoring the optical and the electrical response associated with diverse materials can be also improved by the incorporation of NPs capable of changing electrical and optical interactions. Regarding the contribution of the absorptive nonlinearities to the electrical properties of the studied samples, potential applications for developing optoelectronic nanosystems based on decorated CNTs can be contemplated.

4. Conclusion

A noticeable enhancement in the electrical and photoconductive response exhibited by f-MWCNTs nanotubes was achieved by platinum decoration. Apparently, the incorporation of platinum NPs into MWCNTs originates a modification in the nonresonant electronic levels that can play an important role in the resulting photoconductive and two-photon absorption effects. A simple mechanooptic effect based on the photoconductive response exhibited by the studied samples was observed.

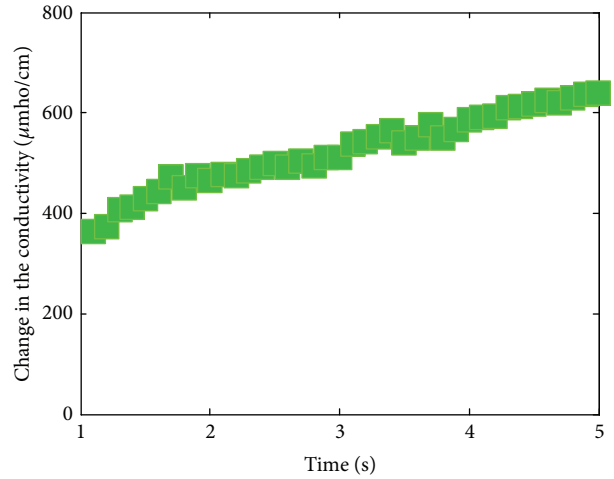

Figure 10: Photoconductive response dependent on nanosecond irradiation in Pt/f-MWCNTs.

Conflict of Interests

The authors declare that there is no conflict of interests regarding the publication of this paper.

Acknowledgments

The authors kindly acknowledge the financial support from the Instituto Politécnico Nacional, Universidad Iberoamericana, and CONACYT. The authors are also thankful to the Centro de Nanociencias y Micro y Nanotecnologías-IPN.

References

[1] A. K. Cuentas-Gallegos, R. Martínez-Rosales, M. E. Rincón, G. A. Hirata, and G. Orozco, "Design of hybrid materials based on carbon nanotubes and polyoxometalates," *Optical Materials*, vol. 29, no. 1, pp. 126–133, 2006.

[2] F. Galantini, S. Bianchi, V. Castelvetro, and G. Gallone, "Functionalized carbon nanotubes as a filler for dielectric elastomer composites with improved actuation performance," *Smart Materials and Structures*, vol. 22, Article ID 05505, 2013.

[3] J. N. Coleman, U. Khan, W. J. Blau, and Y. K. Gun'ko, "Small but strong: a review of the mechanical properties of carbon nanotube-polymer composites," *Carbon*, vol. 44, no. 9, pp. 1624–1652, 2006.

[4] D. Carey, "Editorial: Carbon based electronic," *Journal of Materials Science: Materials in Electronics*, vol. 17, no. 6, pp. 397–398, 2006.

[5] E. Feria-Reyes, C. Torres-Torres, H. Martínez-Gutiérrez et al., "Mechano-optical modulation and optical limiting by multiwall carbon nanotubes," *Journal of Modern Optics*, vol. 60, no. 16, pp. 1321–1326, 2013.

[6] K. Fujisawa, T. Tojo, H. Muramatsu et al., "Enhanced electrical conductivities of N-doped carbon nanotubes by controlled heat treatment," *Nanoscale*, vol. 3, no. 10, pp. 4359–4364, 2011.

[7] J. M. Romo-Herrera, M. Terrones, H. Terrones, and V. Meunier, "Guiding electrical current in nanotube circuits using structural defects: a step forward in nanoelectronics," *ACS Nano*, vol. 2, no. 12, pp. 2585–2591, 2008.

[8] G. Xosrovashvili and N. E. Gorji, "Numerical simulation of carbon nanotubes/GaAs hybrid PV devices with AMPS-1D," *International Journal of Photoenergy*, vol. 2014, Article ID 784857, 6 pages, 2014.

[9] J. H. Lehman, M. Terrones, E. Mansfield, K. E. Hurst, and V. Meunier, "Evaluating the characteristics of multiwall carbon nanotubes," *Carbon*, vol. 49, no. 8, pp. 2581–2602, 2011.

[10] D. H. Galvan, A. Aguilar-Elguézabal, and G. Alonso, "High resolution TEM studies of carbon nanotubes produced by spray pyrolysis," *Optical Materials*, vol. 29, no. 1, pp. 140–143, 2006.

[11] R. Rizvi, J.-K. Kim, and H. Naguib, "Synthesis and characterization of novel low density polyethylene-multiwall carbon nanotube porous composites," *Smart Materials and Structures*, vol. 18, no. 10, Article ID 104002, 2009.

[12] F. Liu, X. B. Zhang, D. Häussler et al., "TEM characterization of metal and metal oxide particles supported by multi-wall carbon nanotubes," *Journal of Materials Science*, vol. 41, no. 14, pp. 4523–4531, 2006.

[13] B. Wu, Y. Kuang, X. Zhang, and J. Chen, "Noble metal nanoparticles/carbon nanotubes nanohybrids: synthesis and applications," *Nano Today*, vol. 6, no. 1, pp. 75–90, 2011.

[14] T. Koretsune and S. Saito, "Electronic structures and three-dimensional effects of boron-doped carbon nanotubes," *Science and Technology of Advanced Materials*, vol. 9, Article ID 044203, 2008.

[15] U. K. Gautam, P. M. F. J. Costa, Y. Bando et al., "Recent developments in inorganically filled carbon nanotubes: successes and challenges," *Science and Technology of Advanced Materials*, vol. 11, no. 5, Article ID 054501, 2010.

[16] M. A. Mohamed, N. Inami, E. Shikoh, Y. Yamamoto, H. Hori, and A. Fujiwara, "Fabrication of spintronics device by direct synthesis of single-walled carbon nanotubes from ferromagnetic electrodes," *Science and Technology of Advanced Materials*, vol. 9, no. 2, Article ID 025019, 2008.

[17] R. Paul, A. Maity, A. Mitra, P. Kumbhakar, and A. K. Mitra, "Synthesis and study of optical and electrical characteristics of a hybrid structure of single wall carbon nanotubes and silver nanoparticles," *Journal of Nanoparticle Research*, vol. 13, no. 11, pp. 5749–5757, 2011.

[18] R. Sreeja, P. M. Aneesh, K. Hasna, and M. K. Jayaraj, "Linear and nonlinear optical properties of multi walled carbon nanotubes with attached gold nanoparticles," *Journal of the Electrochemical Society*, vol. 158, no. 10, pp. K187–K191, 2011.

[19] K. C. Jena, P. B. Bisht, M. M. Shaijumon, and S. Ramaprabhu, "Study of optical nonlinearity of functionalized multi-wall carbon nanotubes by using degenerate four wave mixing and Z-scan techniques," *Optics Communications*, vol. 273, no. 1, pp. 153–158, 2007.

[20] V. A. Margulis, O. V. Boyarkina, and E. A. Gaiduk, "Non-degenerate optical four-wave mixing in single-walled carbon nanotubes," *Optics Communications*, vol. 249, no. 1-3, pp. 339–349, 2005.

[21] C. Torres-Torres, N. Peréa-López, H. Martínez-Gutiérrez et al., "Optoelectronic modulation by multi-wall carbon nanotubes," *Nanotechnol*, vol. 24, Article ID 045201, 2013.

[22] N. Izard, P. Billaud, D. Riehl, and E. Anglaret, "Influence of structure on the optical limiting properties of nanotubes," *Optics Letters*, vol. 30, no. 12, pp. 1509–1511, 2005.

[23] R. Torres-Torres, "Extracting characteristic impedance in low-loss substrates," *Electronics Letters*, vol. 47, no. 3, pp. 191–193, 2011.

[24] W.-Y. Ko and K.-J. Lin, "Highly conductive, transparent flexible films based on metal nanoparticle-carbon nanotube composites," *Journal of Nanomaterials*, vol. 2013, Article ID 505292, 16 pages, 2013.

[25] Y.-A. Li, N.-H. Tai, S.-K. Chen, and T.-Y. Tsai, "Enhancing the electrical conductivity of carbon-nanotube-based transparent conductive films using functionalized few-walled carbon nanotubes decorated with palladium nanoparticles as fillers," *ACS Nano*, vol. 5, no. 8, pp. 6500–6506, 2011.

[26] Y. Lin, K. A. Watson, M. J. Fallbach et al., "Rapid, solventless, bulk preparation of metal nanoparticle-decorated carbon nanotubes," *ACS Nano*, vol. 3, no. 4, pp. 871–884, 2009.

[27] S. Sahoo, S. Husale, S. Karna, S. K. Nayak, and P. M. Ajayan, "Controlled assembly of Ag nanoparticles and carbon nanotube hybrid structures for biosensing," *Journal of the American Chemical Society*, vol. 133, no. 11, pp. 4005–4009, 2011.

[28] Z. He, J. Chen, D. Liu, H. Zhou, and Y. Kuang, "Electrodeposition of Pt-Ru nanoparticles on carbon nanotubes and their electrocatalytic properties for methanol electrooxidation," *Diamond and Related Materials*, vol. 13, no. 10, pp. 1764–1770, 2004.

[29] Z. He, J. Chen, D. Liu, H. Tang, W. Deng, and Y. Kuang, "Deposition and electrocatalytic properties of platinum nanoparticals on carbon nanotubes for methanol electrooxidation," *Materials Chemistry and Physics*, vol. 85, no. 2-3, pp. 396–401, 2004.

[30] T. Ramulifho, K. I. Ozoemena, R. M. Modibedi, C. J. Jafta, and M. K. Mathe, "Fast microwave-assisted solvothermal synthesis of metal nanoparticles (Pd, Ni, Sn) supported on sulfonated MWCNTs: Pd-based bimetallic catalysts for ethanol oxidation in alkaline medium," *Electrochimica Acta*, vol. 59, pp. 310–320, 2012.

[31] C.-Y. Lu, M.-C. Wei, S.-H. Chang, and M.-Y. Wey, "Study of the activity and backscattered electron image of Pt/CNTs prepared by the polyol process for flue gas purification," *Applied Catalysis A*, vol. 354, no. 1-2, pp. 57–62, 2009.

[32] O. Winjobi, Z. Zhang, C. Liang, and W. Li, "Carbon nanotube supported platinum-palladium nanoparticles for formic acid oxidation," *Electrochimica Acta*, vol. 55, no. 13, pp. 4217–4221, 2010.

[33] L. Li and Y. Xing, "Pt-Ru nanoparticles supported on carbon nanotubes as methanol fuel cell catalysts," *Journal of Physical Chemistry C*, vol. 111, no. 6, pp. 2803–2808, 2007.

[34] L. Qiu, V. G. Pol, Y. Wei, and A. Gedanken, "Sonochemical decoration of multi-walled carbon nanotubes with nanocrystalline tin," *New Journal of Chemistry*, vol. 28, no. 8, pp. 1056–1059, 2004.

[35] W.-Y. Ko, J.-W. Su, C.-H. Guo, and K.-J. Lin, "Extraordinary mechanical flexibility in composite thin films composed of bimetallic AgPt nanoparticle-decorated multi-walled carbon nanotubes," *Carbon*, vol. 50, no. 6, pp. 2244–2251, 2012.

[36] M. Terrones, H. Terrones, F. Banhart, J.-C. Charlier, and P. M. Ajayan, "Coalescence of single-walled carbon nanotubes," *Science*, vol. 288, no. 5469, pp. 1226–1229, 2000.

[37] F. Banhart, "The formation of a connection between carbon nanotubes in an electron beam," *Nano Letters*, vol. 1, no. 6, pp. 329–332, 2001.

[38] C. Jin, K. Suenaga, and S. Iijima, "Plumbing carbon nanotubes," *Nature Nanotechnology*, vol. 3, no. 1, pp. 17–21, 2008.

[39] J. A. Rodriguez-Manzo, F. Banhart, M. Terrones et al., "Heterojunctions between metals and carbon nanotubes as ultimate nanocontacts," *Proceedings of the National Academy of Sciences of the United States of America*, vol. 106, no. 12, pp. 4591–4595, 2009.

[40] R. Andrews, D. Jacques, A. M. Rao et al., "Continuous production of aligned carbon nanotubes: a step closer to commercial realization," *Chemical Physics Letters*, vol. 303, no. 5-6, pp. 467–474, 1999.

[41] A. Hirsch and O. Vostrowsky, "Functionalization of carbon nanotubes," *Topics in Current Chemistry*, vol. 245, pp. 193–237, 2005.

[42] R. O. DiLeo, B. J. Landi, and R. P. Rafaelle, "Purity assessment of multiwalled carbon nanotubes by Raman spectroscopy," *Journal of Applied Physics*, vol. 101, no. 6, Article ID 064307, 2007.

[43] C. Mercado-Zuniga, J. R. Vargas-Garcia, F. Cervantes-Sodi, M. Trejo-Valdez, R. Torres-Martinez, and C. Torres-Torres, "Photoconductive logic gate based on platinum decorated carbon nanotubes," *Applied Optics*, vol. 52, no. 22, pp. E22–E27, 2013.

[44] V. Yannopapas, "Enhancement of nonlinear susceptibilities near plasmonic metamaterials," *Optics Communications*, vol. 283, no. 8, pp. 1647–1649, 2010.

[45] M. Trejo-Valdez, C. Torres-Torres, J. H. Castro-Chacon, G. A. Graciano-Armenta, C. I. Garcia-Gil, and A. V. Khomenko, "Modification of the picosecond optical absorptive nonlinearity by a nanosecond irradiation in a nanostructured ZnO thin film," *Optics and Laser Technology*, vol. 49, pp. 75–80, 2013.

[46] W. M. Jacobs, D. A. Nicholson, H. Zemer, A. N. Volkov, and L. V. Zhigilei, "Acoustic energy dissipation and thermalization in carbon nanotubes: atomistic modeling and mesoscopic description," *Physical Review B*, vol. 86, Article ID 165414, 2012.

[47] M. VonAllmen and A. Blatter, *Laser-Beam Interaction with Materials*, Springer, Berlin, Germany, 1995.

[48] D. J. Yang, Q. Zhang, G. Chen et al., "Thermal conductivity of multiwalled carbon nanotubes," *Physical Review B*, vol. 66, no. 16, Article ID 165440, 6 pages, 2002.